

Is Matching Pursuit Solving Convex Problems?

Mingkui Tan, Ivor W. Tsang, and Li Wang

Abstract—Sparse recovery (SR) has emerged as a very powerful tool for signal processing, data mining and pattern recognition. To solve SR, many efficient matching pursuit (MP) algorithms have been proposed. However, it is still not clear whether SR can be formulated as a convex problem that is solvable using MP algorithms. To answer this, in this paper, a novel convex relaxation model is presented, which is solved by a general matching pursuit (GMP) algorithm under the convex programming framework. GMP has several advantages over existing methods. At first, it solves a convex problem and guarantees to converge to a optimum. In addition, with ℓ_1 -regularization, it can recover any k -sparse signals if the restricted isometry constant $\sigma_k \leq 0.307 - \nu$, where ν can be arbitrarily close to 0. Finally, when dealing with a batch of signals, the computation burden can be much reduced using a batch-mode GMP. Comprehensive numerical experiments show that GMP achieves better performance than other methods in terms of sparse recovery ability and efficiency. We also apply GMP to face recognition tasks on two well-known face databases, namely, *Extended using* and *AR*. Experimental results demonstrate that GMP can achieve better recognition performance than the considered state-of-the-art methods within acceptable time. Particularly, the batch-mode GMP can be up to 500 times faster than the considered ℓ_1 methods.

Index Terms—Sparse recovery, compressive sensing, matching pursuit, convex programming, face recognition.

1 INTRODUCTION

Sparse recovery (SR), also known as sparse representation or sparse reconstruction, has been widely used in many applications, such as signal processing and machine learning [1], [2], [3]. Typically, SR is a fundamental element of the compressive sensing [1], [4]. Besides, SR has been successfully applied to image processing tasks, such as image restoration [5], [6], image super-resolution [7] and so on. In machine learning area, SR has been widely applied in robust face recognition [2], subspace clustering [8], [9], dictionary learning [10], [11] and feature learning [3], [12].

From the compressive sensing theory [1], SR guarantees to recover a sparse signal from underdetermined linear systems under some restricted conditions. Consider a linear model $\mathbf{b} = \mathbf{A}\mathbf{x} + \mathbf{e}$, where $\mathbf{A} = [\mathbf{a}_1, \dots, \mathbf{a}_m] \in \mathbb{R}^{n \times m} (n \ll m)$ is a design matrix or dictionary, $\mathbf{a}_j \in \mathbb{R}^n$ denotes the j th atom and $\mathbf{e} \in \mathbb{R}^n$ is the additive noise, SR aims to recover a k -sparse signal \mathbf{x} from \mathbf{b} by solving the following ℓ_0 -norm constrained inverse problem:

$$\min_{\mathbf{x}} \|\mathbf{b} - \mathbf{A}\mathbf{x}\|^2 \quad \text{s.t.} \quad \|\mathbf{x}\|_0 \leq k, \quad (1)$$

where $\|\cdot\|$ and $\|\cdot\|_0$ denote the ℓ_2 and ℓ_0 norm, respectively. Here \mathbf{x} is called as the sparse representation of \mathbf{b} . However, to successfully recover the sparse signals from the the measurement, restricted conditions are necessary. The restricted isometry property (RIP) is one of the important conditions [4]. Specifically, for an $n \times m$ design matrix \mathbf{A} and an integer $k \in [1, m]$, the k -restricted isometry constant $\delta_k \in [0, 1)$ is the smallest number such that,

$$(1 - \delta_k)\|\mathbf{x}\|^2 \leq \|\mathbf{A}\mathbf{x}\|^2 \leq (1 + \delta_k)\|\mathbf{x}\|^2, \quad (2)$$

for all \mathbf{x} with $\|\mathbf{x}\|_0 \leq k$. Studies have shown that it is possible to recover \mathbf{x} with $n = O(k \log(m))$ *nonadaptive*

measurements by solving (1) [1], [4], [13]. However, because of the ℓ_0 -norm constraint, problem (1) is NP-hard to solve [14]. Therefore, practitioners usually solve the its ℓ_1 -convex relaxations [15], [16].

$$\min_{\mathbf{x}} \|\mathbf{x}\|_1 \quad \text{s.t.} \quad \mathbf{b} - \mathbf{A}\mathbf{x} \in \mathcal{B}^p, \quad (3)$$

where \mathcal{B}^p is determined by the noise structure with $p \in \{0, 2, \infty\}$ [17]. Specifically, $\mathcal{B}^0 = \{\mathbf{0}\}$ represents the noiseless case, $\mathcal{B}^2 = \{\boldsymbol{\xi} : \|\boldsymbol{\xi}\| \leq \varepsilon\}$ denotes the ℓ_2 -norm noise, and $\mathcal{B}^\infty = \{\boldsymbol{\xi} : \|\mathbf{A}^\top \boldsymbol{\xi}\|_\infty \leq \lambda\}$ denotes the Dantzig selector [18], [17], respectively. The recovery conditions of ℓ_1 -relaxation have been widely studied by many researchers [1], [4], [13], [17]. For example, [17] shows that if σ_k satisfies $\sigma_k \leq 0.307$, the solution to (3) can recover the k -sparse signals exactly. Let λ be a regularization parameter, in practice, the following ℓ_1 -regularized LASSO problem is also widely studied [19]:

$$\min_{\mathbf{x}} \lambda \|\mathbf{x}\|_1 + \frac{1}{2} \|\mathbf{b} - \mathbf{A}\mathbf{x}\|^2, \quad (4)$$

The major issue of ℓ_1 -relaxations is the unbearable computational cost [20], [21], [22]. Although many fast algorithms have been proposed recently, they are still expensive due to the frequent calculations of $\mathbf{A}\mathbf{x}$ and $\mathbf{A}^\top \boldsymbol{\xi}$ [23]. In real-world applications, to make it solvable with acceptable cost, the number of n has to be reduced using random projections or PCA [2], [21]. However, with dimension reduction, the recognition performance may decrease [21]. Typically, two recent papers argued that the simple least square regression (denote by L2) or the ℓ_2 -regularized least square regression (denote by L2-L2) can achieve better recognition rates and faster recognition speed than SR on face recognition tasks without dimension reduction [21], [22]. Furthermore, since the solutions of L2 and L2-L2 are not sparse but provide comparable performance, the authors argued that the enforcing of sparsity constraints may not help improve the recognition performance but bring heavy computational cost [20], [21], [22].

Regardless of the arguments on the effectiveness of sparsity, the heavy computational cost of solving ℓ_1 -relaxations is

• Mingkui Tan and Ivor W. Tsang are with the School of Computer Engineering, Nanyang Technological University, 639798, Singapore. e-mail: {tanm0097, IvorTsang, yzhai1}@e.ntu.edu.sg.

• Li Wang is with the Department of Mathematics, University of California, San Diego, CA 92093, USA. e-mail: liw022@ucsd.edu.

widely acknowledged [2], [20], [21], [22]. Accordingly, how to improve the efficiency of SR is an urgent issue. Besides ℓ_1 -convex relaxations, matching pursuit (MP) includes another family of SR methods [24], [25], [23]. Among them, the orthogonal matching pursuit (OMP) or the fully corrective forward greedy selection (FCFGS) is the most well known [26], [27]. The greedy idea of OMP has also been extended to solve more general sparse problems with slight modifications [28], [29]. Unfortunately, these OMP type methods, which only include one atom in each iteration, are very expensive for computation especially when the sparsity k is large.

To improve the efficiency, many OMP variants have been proposed, including the regularized orthogonal matching pursuit (ROMP) [30], compressive sampling matching pursuit (CoSaMP) [24], subspace pursuit (SP) [25], accelerated iterative hard thresholding (AIHT) [31], [32], [33], orthogonal matching pursuit with replacement (OMPR) [23] and so on. For these variants, the computational cost can be much reduced since they only calculate $\mathbf{A}^\top \boldsymbol{\xi}$ several times [23]. Therefore, they are more attractive when solving large-scale problems. The convergence and recovery conditions of these algorithms have also been thoroughly studied, which are usually expressed as RIP constants [24], [25], [23]. Typically, CoSaMP, SP, AIHT and OMPR can recover any k -sparse signal provided with $\delta_{4k} < 0.35$, $\delta_{3k} < 0.35$, $\delta_{3k} < 1/\sqrt{32}$ and $\delta_{2k} < 0.499$, respectively [23].

However, the major disadvantage of the above OMP variants (except AIHT) is that the recovery conditions are also their corresponding convergence guarantees. In other words, if these conditions do not hold, their convergence cannot be guaranteed. While the RIP conditions are not difficult to satisfy in compressive sensing, it may be too strict to achieve in real-world applications. For example, in the face recognition tasks, several images of the same person may be highly correlated. In this case, δ_{tk} can be very large even for small k , where $t \geq 1$ is an integer. In other words, the RIP conditions will be violated. Consequently, the above improved OMP variants may not converge¹. Another disadvantage of the OMP variants is that, most of them, such as SP, require a good estimation of the sparsity k ; otherwise, their performance will decrease. Unfortunately, in real-world applications, the estimation of ground-truth sparsity is not trivial, which restricted the applications of these methods.

Regarding the computational issue of ℓ_1 -convex relaxations and OMP type methods, and the convergence issue of the improved OMP variants, the core contributions of this paper are summarized as follows:

- We propose a new convex relaxation for sparse recovery. To solve the new relaxation, a general matching pursuit (GMP) algorithm, which includes the standard OMP as a special case, is introduced. Since GMP solves a convex problem, its convergence is guaranteed. In addition, GMP does not need to specify the estimation of the target sparsity, which is desired in many real-world applications. Finally, a subspace exploratory matching is presented to

further improve the performance of GMP.

- We show that with ℓ_1 regularizer, GMP guarantees to recover any k -sparse signals if $\delta_k \leq 0.307 - \nu$, where ν can be arbitrarily close to 0. Furthermore, under mild conditions, GMP can exponentially converge to the optimal solution. A collection of numerical experiments demonstrate the effectiveness and efficiency of GMP on sparse recovery problems.
- The sure convergence facilitates GMP for many real-world applications. In this paper, we apply GMP to face recognition tasks. Experimental results on two well-known face datasets, namely *Extended using* and *AR* databases, show that GMP with **batch mode implementation** achieves better recognition rates than L2 and L2-L2 methods with comparable computational cost. Particularly, it can be up to 500 times faster than the state-of-the-art ℓ_1 solver.

The rest of this paper is organized as follows. In Section 2, a new convex relaxation for sparse recovery is presented. To solve this relaxation, in Section 3, we propose a general matching pursuit algorithm with detailed analysis. The related work is discussed in Section 4. Numerical experiments and the application of GMP to face recognition are shown in Section 5 and 6, respectively. Conclusive remarks will be given in Section 7. Besides, all the technical proofs of this paper are shown in **supplementary files**.

2 A NEW CONVEX RELAXATION MODEL FOR SPARSE RECOVERY

2.1 Notations and Preliminaries

Throughout the paper, we denote the transpose of vector/matrix by the superscript \top , $\mathbf{0}$ as a zero vector and $\text{diag}(\mathbf{v})$ as a diagonal matrix with diagonal entries equal to \mathbf{v} . In addition, we denote $\|\mathbf{v}\|_p$ and $\|\mathbf{v}\|$ as the ℓ_p -norm and ℓ_2 -norm of a vector \mathbf{v} , respectively. For a function $f(\mathbf{x})$, we denote by $\nabla f(\mathbf{x})$ and $\partial f(\mathbf{x})$ as the gradient and subgradient of $f(\mathbf{x})$ at \mathbf{x} , respectively. For a sparse vector \mathbf{x} , let the calligraphic letter $\mathcal{T} = \text{support}(\mathbf{x}) = \{i | x_i \neq 0\} \in \{1, \dots, m\}$ denote its support [17] and $\mathbf{x}_{\mathcal{T}}$ be the subvector indexed by \mathcal{T} . Furthermore, let \mathcal{T}^c be the complementary set of \mathcal{T} , i.e. $\mathcal{T}^c = \{1, \dots, m\} \setminus \mathcal{T}$. Finally, let $\mathbf{A} \odot \mathbf{B}$ represent the element-wise product of two matrices \mathbf{A} and \mathbf{B} . We also need the following definition of *Restricted Eigenvalue Condition*, *Restricted Condition Number* and *Restricted Set*.

Definition 1. [19] Given an integer $k > 0$, a design matrix \mathbf{A} is said to satisfy the *Restricted Eigenvalue Condition* at sparsity level k , if there exists positive constants $\gamma_-(\mathbf{A}, k)$ and $\gamma_+(\mathbf{A}, k)$ such that

$$\gamma_-(\mathbf{A}, k) = \inf \left\{ \frac{\mathbf{x}^\top \mathbf{A}^\top \mathbf{A} \mathbf{x}}{\mathbf{x}^\top \mathbf{x}}, \mathbf{x} \neq \mathbf{0}, \|\mathbf{x}\|_0 \leq k \right\}, \quad (5)$$

$$\gamma_+(\mathbf{A}, k) = \sup \left\{ \frac{\mathbf{x}^\top \mathbf{A}^\top \mathbf{A} \mathbf{x}}{\mathbf{x}^\top \mathbf{x}}, \mathbf{x} \neq \mathbf{0}, \|\mathbf{x}\|_0 \leq k \right\}. \quad (6)$$

In addition, the *Restricted Condition Number* is defined as

$$\kappa(\mathbf{A}, k) = \frac{\gamma_+(\mathbf{A}, k)}{\gamma_-(\mathbf{A}, k)}. \quad (7)$$

Lemma 1. Let $k \leq k'$, then we have $\gamma_+(\mathbf{A}, k) \leq \gamma_+(\mathbf{A}, k')$, $\gamma_-(\mathbf{A}, k) \geq \gamma_-(\mathbf{A}, k')$ and $\kappa(\mathbf{A}, k) \leq \kappa(\mathbf{A}, k')$.

1. An experiment on a non-RIP toy problem will be given in Section 5.2.3 (shown as in Fig. 3) to demonstrate this issue.

Definition 2. Restricted Set [34]. Given an index set \mathcal{T} , the restricted set is defined as $\Gamma_D = \{\mathbf{h} \in \mathbb{R}^m : \|\mathbf{h}_{\mathcal{T}^c}\|_1 \leq D\|\mathbf{h}_{\mathcal{T}}\|_1\}$, where \mathcal{T}^c denotes the complementary set of \mathcal{T} .

2.2 A New Convex Relaxation Model

Notice that SR can be considered as a support detection problem [23]. Motivated by this fact, we introduce a support selection vector $\boldsymbol{\tau} \in \{0, 1\}^m$ to select the atoms, where the i th atom is selected if and only if $\tau_i = 1$. In addition, to enforce the sparsity, we impose a sparsity constraint $\|\boldsymbol{\tau}\|_0 \leq \varrho < k$ to control the number of selected atoms. Here we use ϱ to distinguish the target sparsity k in equation (1) for that ϱ is only a conservative estimation (namely, ϱ can be several times smaller than k) to the ground-truth sparsity, which is often unknown in advance in real-world problems.

With the introduction of the support selection vector $\boldsymbol{\tau}$, we now give a new model for SR. For simplicity, let $\Lambda = \{\boldsymbol{\tau} : \|\boldsymbol{\tau}\|_0 \leq \varrho, \boldsymbol{\tau} \in \{0, 1\}^m\}$ be the domain of $\boldsymbol{\tau}$ and for each $\boldsymbol{\tau} \in \Lambda$, $\mathbf{A}\text{diag}(\boldsymbol{\tau})\mathbf{x} = \mathbf{A}(\boldsymbol{\tau} \odot \mathbf{x})$. Let $\boldsymbol{\xi} = \mathbf{b} - \mathbf{A}(\boldsymbol{\tau} \odot \mathbf{x})$ be the regression error, based on the formulation (4), we consider to solve an alternative model:

$$\begin{aligned} M1 : \quad & \min_{\boldsymbol{\tau} \in \Lambda} \min_{\mathbf{x}, \boldsymbol{\xi}} \lambda \|\mathbf{x}\|_1 + \frac{1}{2} \|\boldsymbol{\xi}\|^2 \\ \text{s.t.} \quad & \boldsymbol{\xi} = \mathbf{b} - \mathbf{A}(\mathbf{x} \odot \boldsymbol{\tau}), \|\boldsymbol{\tau}\|_0 \leq \varrho. \end{aligned} \quad (8)$$

It is also interesting to solve the following problem by setting $\lambda = 0$.

$$\begin{aligned} M2 : \quad & \min_{\boldsymbol{\tau} \in \Lambda} \min_{\mathbf{x}, \boldsymbol{\xi}} \frac{1}{2} \|\boldsymbol{\xi}\|^2 \\ \text{s.t.} \quad & \boldsymbol{\xi} = \mathbf{b} - \mathbf{A}(\mathbf{x} \odot \boldsymbol{\tau}), \|\boldsymbol{\tau}\|_0 \leq \varrho. \end{aligned} \quad (9)$$

As $M2$ is a special case of $M1$, hereafter we will not differentiate them unless specified. Note that in both (8) and (9), there are $\sum_{i=0}^{\varrho} \binom{m}{i}$ feasible $\boldsymbol{\tau}$ in Λ . The tasks of the optimization problems in (8) and (9) are to find the **BEST** $\boldsymbol{\tau}$ from the feasible set to minimize the regression loss $\|\boldsymbol{\xi}\|^2$. Unfortunately, these two optimization problems are very difficult to solve due to the exponential number of constraints. To make them solvable, we firstly conduct the following transformations.

Proposition 1. By introducing the dual form of the inner minimization problem, Problem (8) can be reformulated as

$$\begin{aligned} \min_{\boldsymbol{\alpha}} \max_{\boldsymbol{\alpha}} \quad & -\frac{1}{2} \|\boldsymbol{\alpha}\|^2 + \boldsymbol{\alpha}^\top \mathbf{b} \\ \text{s.t.} \quad & \|\boldsymbol{\alpha}^\top \mathbf{A}\text{diag}(\boldsymbol{\tau})\|_\infty \leq \lambda, \|\boldsymbol{\tau}\|_0 \leq \varrho, \end{aligned} \quad (10)$$

where $\boldsymbol{\alpha} = \boldsymbol{\xi}$ is the dual variable to the constraint $\boldsymbol{\xi} = \mathbf{b} - \mathbf{A}(\mathbf{x} \odot \boldsymbol{\tau})$. If $\lambda = 0$, the constraint becomes $\boldsymbol{\alpha}^\top \mathbf{A}\text{diag}(\boldsymbol{\tau}) = \mathbf{0}$, $\|\boldsymbol{\tau}\|_0 \leq \varrho$ for $M2$. Finally, let \mathbf{x}^* be the optimal solution of problem $M1$ or $M2$, then $x_j^* = 0$ if $\tau_j = 0$.

In Proposition 1, we have $\boldsymbol{\alpha} = \boldsymbol{\xi}$ at the optimality, which is particularly important in the following derivations. At first, as the regression error $\boldsymbol{\xi}$ is always bounded, we have $\boldsymbol{\xi} = \mathbf{b}$ for $\mathbf{x} = \mathbf{0}$. Without loss of generality, we can define a feasible domain for $\boldsymbol{\alpha}$ w.r.t. a feasible $\boldsymbol{\tau}$ as $\mathcal{A}_\tau^\lambda = \{\boldsymbol{\alpha} : \|\boldsymbol{\alpha}^\top \mathbf{A}\text{diag}(\boldsymbol{\tau})\|_\infty \leq \lambda, \boldsymbol{\alpha} \in [-l, l]^n\}$ to (10). Here $l > 0$ is a large number such that the optimal solution $\boldsymbol{\alpha}^*$ always exists and is achievable in the defined domain. In addition, we define:

$$f(\boldsymbol{\alpha}, \boldsymbol{\tau}) = \frac{1}{2} \|\boldsymbol{\alpha}\|^2 - \boldsymbol{\alpha}^\top \mathbf{b}, \quad \boldsymbol{\alpha} \in \mathcal{A}_\tau^\lambda. \quad (11)$$

Moreover, for a given $\boldsymbol{\tau}$, define by $\max_{\boldsymbol{\alpha}} -f(\boldsymbol{\alpha}, \boldsymbol{\tau})$ as the maximizer over $\boldsymbol{\alpha}$ and $\min_{\boldsymbol{\tau} \in \Lambda} \max_{\boldsymbol{\alpha}} -f(\boldsymbol{\alpha}, \boldsymbol{\tau}) = \min_{\boldsymbol{\tau} \in \Lambda} (\max_{\boldsymbol{\alpha}} -f(\boldsymbol{\alpha}, \boldsymbol{\tau}))$ as the minimizer among all possible $\boldsymbol{\tau} \in \Lambda$. Since $|\Lambda|$ is finite, the minimizer is always achievable by enumeration. However, this enumeration process will become computationally intractable for large m and ϱ , in which $|\Lambda|$ becomes extremely huge. Fortunately, we can make the convex relaxation to (10) according to the following theorem.

Theorem 1. (Convex relaxation) With \mathcal{A}_τ^λ and Λ defined above, we have

$$\min_{\boldsymbol{\tau} \in \Lambda} \max_{\boldsymbol{\alpha}} -f(\boldsymbol{\alpha}, \boldsymbol{\tau}) \geq \max_{\boldsymbol{\alpha}} \min_{\boldsymbol{\tau} \in \Lambda} -f(\boldsymbol{\alpha}, \boldsymbol{\tau}). \quad (12)$$

Notice that the latter problem in formulation (12) is the convex relaxation to $\min_{\boldsymbol{\tau} \in \Lambda} \max_{\boldsymbol{\alpha}} -f(\boldsymbol{\alpha}, \boldsymbol{\tau})$, which can be further transformed as a QCQP problem.

Proposition 2. (QCQP for SR). By introducing a new variable $\theta \in \mathbb{R}$, $\max_{\boldsymbol{\alpha}} \min_{\boldsymbol{\tau} \in \Lambda} -f(\boldsymbol{\alpha}, \boldsymbol{\tau})$ is equivalent to a convex QCQP problem [35]:

$$\min_{\boldsymbol{\alpha}, \theta} \quad \theta : \text{s.t.} \quad f(\boldsymbol{\alpha}, \boldsymbol{\tau}) \leq \theta, \quad \forall \boldsymbol{\tau} \in \Lambda, \boldsymbol{\alpha} \in \mathcal{A}_\tau^\lambda. \quad (13)$$

In the rest of the paper, we will focus on solving the QCQP problem (13) for SR. Unfortunately, since the number of constraints is as many as $\sum_{i=0}^{\varrho} \binom{m}{i}$, it will become very huge for median size m and ϱ , making (13) intractable. Therefore, how to solve it efficiently is our core concern in the following sections.

3 GENERAL MATCHING PURSUIT

Although there are $\sum_{i=0}^{\varrho} \binom{m}{i}$ constraints defined in Λ , the intrinsic sparsity of the SR problem ensures that the number of active constraints is very small. Ideally, for the k -sparse signal \mathbf{x} , there exists at least $\lceil k/\varrho \rceil$ optimal $\boldsymbol{\tau}$'s such that the support of \mathbf{x} can be included by these $\boldsymbol{\tau}$'s. In other words, the number of active $\boldsymbol{\tau}$'s is very small. The question is: how can we gradually infer these active $\boldsymbol{\tau}$'s from the exponential number of candidates?

Notice that, problem (13) can be considered as a special case of the semi-infinite programming (SIP) problem [36]. Since the SIP problem can be efficiently addressed by a central cutting plane (CCP) algorithm [36], we seek to address (13) by adopting CCP algorithm. Follow [36], the details of the CCP algorithm for solving (13) are described in Algorithm 1.

Algorithm 1 Central cutting plane method for (13).

0: Initialize $\boldsymbol{\alpha}^0 = \mathbf{b}$, and do **worst-case analysis** to find the most-violated constraint $\boldsymbol{\tau}_0$.

1: Let $\theta^0 = f(\boldsymbol{\alpha}^0, \boldsymbol{\tau}_0)$, $\Lambda_0 = \{\boldsymbol{\tau}_0\}$ and $t = 1$.

2: Solve the following program:

$$\max_{\boldsymbol{\alpha}, \delta} \delta \text{ s.t. } \theta + \delta \leq \theta^{t-1}, f(\boldsymbol{\alpha}, \boldsymbol{\tau}_t) \leq \theta - \delta, \forall \boldsymbol{\tau}_t \in \Lambda_{t-1}. \quad (14)$$

3: Let $(\boldsymbol{\alpha}^t, \theta^t, \delta^t)$ be the solution to (14). If the stopping condition achieves, stop.

4: Obtain a new violated constraint $\boldsymbol{\tau}_t$ by **worst-case analysis**.

5: Set $\Lambda_t = \Lambda_{t-1} \cup \{\boldsymbol{\tau}_t\}$. If $f(\boldsymbol{\alpha}^t, \boldsymbol{\tau}_t) > \theta^t$, that is, $\boldsymbol{\alpha}^t$ is an infeasible solution to (13), and then add the constraint $f(\boldsymbol{\alpha}, \boldsymbol{\tau}_t) \leq \theta - \delta$ to SD_t . Let $t = t + 1$ and go to Step 2.

The basic idea of Algorithm 1 is: instead of solving the SIP with all constraints defined by Λ , it iteratively finds one possible **active constraint** through worst-case analysis and adds it into the active constraint set Λ_t that is initialized as \emptyset . After that, the master problem (14) with active constraints will be solved. An important issue for the worst-case analysis is the initial guess of α^0 . Typically, since $\mathbf{x}^0 = \mathbf{0}$ holds at the initial stage, we have $\xi = \mathbf{b}$. Accordingly, the dual variable α^0 can be set by $\alpha^0 = \mathbf{b}$. Interested readers can refer to [37], [36] for the detailed discussions of this algorithm. The details of the worst-case analysis, the solution to the master problem and the stopping conditions will be discussed in the following subsections.

3.1 Worst-Case Analysis

In Algorithm 1, the first step is to find the most active τ from the exponential number candidates, which is named as the worst-case analysis. Recall that, at the optimality of (13), the following conditions should hold:

$$\|\alpha^\top \mathbf{A} \text{diag}(\tau)\|_\infty \leq \lambda. \quad (15)$$

Let $\mathbf{g} = \mathbf{A}^\top \alpha$, apparently, any atom \mathbf{a}_i with $|g_i| > \lambda$ violates the optimality condition and the atom with the largest $|g_i|$ violates the condition the most. Since $|\tau|_0 \leq \varrho$, the ϱ atoms with the largest $|g_i|$ will form an active constraint. To be more specific, to obtain the most-active τ_t , we can set the ϱ entries of τ_t with the largest $|g_i|$ to 1 and the rests to 0.

Recall that this strategy is akin to the matching step in traditional MP algorithms [24], [23], [26]. Therefore, we refer Algorithm 1 as general matching pursuit (GMP) algorithm. The effectiveness as well as the deficiency of the worst-case analysis will be further studied later.

3.2 Master Problem Optimization

In Algorithm 2, the second step is to solve the master problem (14) with the selected active constraints. To begin with, we make the following notations. At first, let \mathcal{J}_i be a index set of atoms selected by τ_i , where τ_i includes ϱ active atoms. In the worst-case analysis, it is easy to ensure that there is no overlapping elements among \mathcal{J}_i , for all i . In the following, let $\mathcal{I}_t = \cup_i \mathcal{J}_i$ be the index set of all selected atoms at the t th iteration. Finally, let $T = |\Lambda_t|$ be the size of active constraints for the t th iteration, we have $T \leq t$, where the inequality holds if some non-active constraints are deleted from Λ_t during the optimization [36]. The following lemma indicates that the master problem (14) can be solved in the dual.

Lemma 2. *In the master problem (14) of the t th iteration, let $\{\nu\}$ and $\{\hat{\mu}_i\}$ be the optimal dual variables, and $\boldsymbol{\mu} \in \Pi = \{\boldsymbol{\mu} | \boldsymbol{\mu} \succeq \mathbf{0}, \sum_{i=1}^T \mu_i = 1\}$, problem (14) can be solved in the following dual form:*

$$\min_{\boldsymbol{\mu} \in \Pi} \max_{\boldsymbol{\alpha} \in \mathcal{A}} \frac{1}{2} \theta^{t-1} - \frac{1}{2} \sum_{\tau_i \in \Lambda_t} \mu_i f(\boldsymbol{\alpha}, \tau_i). \quad (16)$$

Unfortunately, it is very difficult to solve the minimax problem (16) directly. Particularly, the computational cost is very expensive if n is very large. Motivated by the fact that, problem (16) only relates to a small set of active atoms, namely

$|\mathcal{I}_t| = T\varrho \ll n$, we seek to solve it w.r.t. the sparse primal variable \mathbf{x} . Fortunately, the following theorem provides such feasibility.

Theorem 2. *Suppose no overlapping elements exist among \mathcal{J}_i and $\mathcal{I}_t = \cup_i \mathcal{J}_i$, problem (16) can be addressed by solving an ℓ_1 -regularized problem with variables ξ and \mathbf{x} w.r.t. the subset \mathcal{I}_t :*

$$\min_{\mathbf{x}, \xi} \lambda \|\mathbf{x}\|_1 + \frac{1}{2} \|\xi\|^2 : \text{s.t. } \xi = \mathbf{b} - \mathbf{A}\mathbf{x}, \quad \mathbf{x}_{\mathcal{I}_t^c} = \mathbf{0}. \quad (17)$$

If $\lambda = 0$, it becomes a least square regression problem. Furthermore, α can be recovered by $\alpha = \xi$.

3.3 GMP in Primal

Now that the master problem can be addressed w.r.t. variables \mathbf{x} and ξ , we can rewrite Algorithm 1 in the primal form. Notice that Algorithm 1 includes two-layer loops: the outer loop for CCP iteration and the inner loop for solving the master problem. To differentiate the two loops, we use t as the outer loop index and k as the inner loop index. Furthermore, we denote by \mathbf{x}^t the outer iteration variable and \mathbf{u}^k the inner iteration variable. Recall that the master problem is defined on the atoms indexed by \mathcal{I}_t , with the relation $\alpha = \xi$, GMP in Algorithm 1 can be implemented in the primal form, which is shown in Algorithm 2.

In Algorithm 2, the master problem is solved by proximal gradient (PG) or conjugate gradient descent (CGD) method [38], [39], which will be depicted later. Moreover, to accelerate the convergence, when doing master problem optimization, we set $\mathbf{u}_{\mathcal{I}_t}^0 = \mathbf{x}_{\mathcal{I}_t}^{t-1}$ as a warm-start. Once the inner optimization is finished, we can set $\mathbf{x}_{\mathcal{I}_t}^t = \mathbf{u}_{\mathcal{I}_t}^k$ and $\mathbf{x}_{\mathcal{I}_t^c}^t = \mathbf{0}$ for the next warm-start, where $\mathbf{u}_{\mathcal{I}_t}^k$ is optimal solution (or approximate optimal solution) obtained by PG or CGD iterations. It is worth mentioning that the computational cost for the master problem optimization takes only $O(n|\mathcal{I}_t|)$, since it is performed on the set \mathcal{I}_t .

Algorithm 2 GMP in primal.

- Initialize $\mathbf{x}^0 = \mathbf{0}$, $\alpha^0 = \mathbf{b}$, $\mathcal{I}_0 = \emptyset$. Let $t = 1$.
 - 1: Do worst-case analysis: Let $\mathbf{g} = \mathbf{A}^\top \alpha^{t-1}$; choose the ϱ largest $|g_j|$ and record their indices by \mathcal{J}_t . Let $\mathcal{I}_t = \mathcal{I}_{t-1} \cup \mathcal{J}_t$.
 - 2: Solve the master problem:
 - Initialize $\mathbf{u}_{\mathcal{I}_t}^0 = \mathbf{x}_{\mathcal{I}_t}^{t-1}$.
 - For $k = 1, \dots$
 - Update $\mathbf{u}_{\mathcal{I}_t}^k$ using PG ($\lambda > 0$) or CGD ($\lambda = 0$) rules.
 - Quit if the stopping condition achieves.
 - End.
 - 3: Let $\mathbf{x}_{\mathcal{I}_t}^t = \mathbf{u}_{\mathcal{I}_t}^k$, $\mathbf{x}_{\mathcal{I}_t^c}^t = \mathbf{0}$ and $\alpha^t = \xi$.
 - 4: Quit if the stopping condition achieves. Otherwise, let $t = t + 1$ and go to step 1.
-

For completeness, now we present the general idea to solve the primal problem (17). Since it is an ℓ_1 -regularized problem, any existing ℓ_1 solver can be adopted to solve it. In this paper, we choose the projected gradient (PG) method since it has attractive convergence properties [38]. Define $\varphi(\mathbf{x}) = \frac{1}{2} \|\mathbf{b} - \mathbf{A}\mathbf{x}\|^2$ and

$$f(\mathbf{x}) = \lambda \|\mathbf{x}\|_1 + \varphi(\mathbf{x}). \quad (18)$$

In PG, it iteratively minimizes the following local quadratic approximation of $f(\mathbf{x})$ at a fixed point \mathbf{u} :

$$\phi(\mathbf{x}, \mathbf{u}) = \lambda \|\mathbf{x}\|_1 + \varphi(\mathbf{u}) + \nabla \varphi(\mathbf{u})^\top (\mathbf{x} - \mathbf{u}) + \frac{L}{2} \|\mathbf{x} - \mathbf{u}\|^2, \quad (19)$$

where L is a positive number. To iterate, PG relies on the soft-thresholding operator: $S_{L,\lambda}(\mathbf{o})_i = \text{sign}(o_i) \max\{|o_i| - \frac{\lambda}{L}, 0\}$. Moreover, let \mathbf{u}^k be the point at the k th iteration of PG and $\mathbf{g} = \nabla \varphi(\mathbf{u}^k) = \mathbf{A}^\top (\mathbf{A}\mathbf{u}^k - \mathbf{b})$, the minimizer of $\phi(\mathbf{x}, \mathbf{u}^k)$ can be calculated by $S_{L,\lambda}(\mathbf{u}^k - \mathbf{g}/L)$. Then the basic updating rule for PG can be written as:

$$\mathbf{u}^{k+1} = S_{L,\lambda}(\mathbf{u}^k - \mathbf{g}/L) = \mathbf{u}^k - 1/LG(\mathbf{u}^k), \quad (20)$$

where $G(\mathbf{u}^k) = L(\mathbf{u}^k - S_{L,\lambda}(\mathbf{u}^k - \mathbf{g}/L))$ is called as the generalized gradient and L can be adjusted by the line search method [38]. Interested readers can refer to [38] for more details.

When $\lambda = 0$, the master problem becomes a least square regression problem and $G(\mathbf{u}^k) = \mathbf{g}$ is the gradient of $\varphi(\mathbf{u}^k)$. Although it can also be solved by PG algorithm, other solvers such as CGD can achieve better efficiency [39] due to two reasons: firstly, the step size in CGD is calculated by the exact line search and the computation cost of the line search in PG can be avoided; secondly, CGD has a better factor for the convergence rate than PG, as shown by the following theorem.

Theorem 3. ([39], [38]) *At the t th iteration of Algorithm 2, if $\gamma_-(\mathbf{A}, t\varrho) > 0$ or $1 - \delta_{t\varrho} > 0$, (namely, the master problem is strongly convex w.r.t. the sub-variables indexed by \mathcal{I}), both PG and CGD have geometric convergence rate w.r.t. the sub-variables $\mathbf{x}_{\mathcal{I}}$. Specifically, let $\{\mathbf{u}^k\}$ be the sequence generated by CGD or PG, \mathbf{u}^* be the minimizer w.r.t. the variables indexed by \mathcal{I}_t and $f(\mathbf{u}^*)$ be the optimal function value, $\frac{f(\mathbf{u}^k) - f(\mathbf{u}^*)}{f(\mathbf{u}^0) - f(\mathbf{u}^*)} \leq \chi^k$ holds. Here, $\chi = (\sqrt{\kappa(\mathbf{Q})} - 1)/(\sqrt{\kappa(\mathbf{Q})} + 1)$ is for CGD and $\chi = \left(1 - \frac{1}{4\eta_u \kappa(\mathbf{Q})}\right)$ is for PG. In addition, according to Lemma 1, χ will gradually increase with increasing t .*

Theorem 3 indicates that both PG and CGD can converge to the optimum after finite iterations if $\gamma_-(\mathbf{A}, t\varrho) > 0$ or $\delta_{t\varrho} > 0$. Moreover, when t goes larger, the factor χ will increase and the computation cost will increase, too.

Now we discuss the relationship between GMP and the standard OMP [26]. Recall that OMP iteratively takes the following three steps. At first, it includes one atom with the largest $|\mathbf{a}_j^\top \mathbf{r}|$ into the support set by $\mathcal{I} = \mathcal{I} \cup \{j\}$, where $\mathbf{r} = \mathbf{b} - \mathbf{A}\mathbf{x}$ is the residual. After that, an orthogonal projection is performed by solving $\min_{\mathbf{x}_{\mathcal{I}}} \frac{1}{2} \|\mathbf{b} - \mathbf{A}_{\mathcal{I}}\mathbf{x}_{\mathcal{I}}\|^2$. Finally, the residual \mathbf{r} is updated by $\mathbf{r} = \mathbf{b} - \mathbf{A}_{\mathcal{I}}\mathbf{u}_{\mathcal{I}}$. We can observe that OMP is a special case of GMP when $\lambda = 0$ and $\varrho = 1$.

Remark 1. *The classical OMP algorithm solves the convex problem (13) regarding M2 with $\varrho = 1$ and $\lambda = 0$.*

3.4 Subspace Exploratory Matching

Now we study the effectiveness of the worst-case analysis. First of all, it is interesting to measure the progress of each outer loop in GMP after the worst-case analysis. Typically, we have the following result.

Lemma 3. *Let $G(\mathbf{x}^t)$ be the generalized gradient at \mathbf{x}^t and $\mathbf{g} = \nabla \varphi(\mathbf{x}^t)$, \mathcal{J}_{t+1} be the index set of atoms selected by the worst-case analysis and \mathbf{u}^1 be the point after the first iteration of the inner loop, with proper line search, we have:*

$$f(\mathbf{x}^t) - f(\mathbf{u}^1) \geq \frac{1}{2L} \|G_{\mathcal{J}_{t+1}}(\mathbf{x}^t)\|^2 = \frac{1}{2L} \sum_{i \in \mathcal{J}_{t+1}} (|g_i| - \lambda)^2. \quad (21)$$

where $|g_i| > \lambda$ for $\forall i \in \mathcal{J}_{t+1}$.

From Lemma 3, on the one hand, it indicates that, the selection of the ϱ elements with the largest $|g_i|$ can achieve the best *lower bound* on the objective value improvement for the first iteration of the inner loop. In other words, the worst-case analysis is effective.

Algorithm 3 Subspace Exploratory Matching.

```

0: Give dictionary  $\mathbf{A}$  and  $\omega (\omega \geq 1)$ , initialize  $\boldsymbol{\alpha} = \mathbf{b}$ .
1: Calculate  $\mathbf{g} = \mathbf{A}^\top \boldsymbol{\alpha}$ . Choose the  $\omega\varrho$  atoms with the largest  $|g_j|$ 's and record the indices in set  $\mathcal{J}_\omega$ . Let  $\mathcal{I}_\omega = \mathcal{I}_t \cup \mathcal{J}_\omega$ .
2: Solve the master problem:
   Initialize  $\mathbf{u}_{\mathcal{I}_\omega}^0 = \mathbf{x}_{\mathcal{I}_\omega}^{t-1}$ .
   For  $k = 1, \dots$ ,
     Update  $\mathbf{u}_{\mathcal{I}_\omega}^k$  using PG (for M1) or CGD (for M2).
     Quit if the stopping condition achieves.
   End.
3: Sort those  $\omega\varrho$  atoms by their regressors  $|u_i|$  in descending order and return the first  $\varrho$  atoms.
```

On the other hand, this *lower bound* cannot be guaranteed for more inner iterations. Therefore, it may be suboptimal when ϱ is relatively large, where some non-support atoms may be wrongly included. To address this issue, we can explore a larger search space. To be more specific, we can seek to include $\omega\varrho$ ($\omega > 1$) elements with the largest $|g_i|$ and then solve the master problem with all selected atoms. Finally, we only select the ϱ atoms with larger regressors from the new atoms. This scheme, named as subspace exploratory matching, is summarized in Algorithm 3. With the subspace search, the convergence speed as well as the decoding performance can be improved. However, additional computational cost will be consumed to solve the master problem. Fortunately, since the inner master problem solver can geometrically converge, several iterations will be enough with warm-start. Finally, to distinguish the two matching schemes, hereafter we term the GMP with subspace search as SGMP.

3.5 Stopping Conditions

The stopping condition is important for MP algorithms. With properly selected λ^2 , a natural stopping condition for GMP is

$$\|\boldsymbol{\alpha}^\top \mathbf{A}\|_\infty \leq \lambda. \quad (22)$$

However, when λ is arbitrarily small, GMP will converge to the point where $\|\boldsymbol{\alpha}\| < \|\boldsymbol{\xi}\|$, where $\boldsymbol{\xi}$ is the noise. Apparently, this is meaningless. The same problem also exists in OMP. To address this issue in OMP, [41] proposes two stopping conditions:

$$\|\boldsymbol{\alpha}^\top \mathbf{A}\|_\infty \leq r_\infty \quad \text{and} \quad \|\boldsymbol{\alpha}\| \leq r_2, \quad (23)$$

2. The selection of the regularization parameter λ depends on the structure of the noises [40], which is beyond the scope of this paper.

where $r_\infty > 0$ and $r_2 > 0$ are pre-determined value based on the structures of different noises [41]. These two conditions are also applicable for GMP. However, in real applications, it is not easy to obtain the noise structures, making the setting of r_∞ or r_2 difficult. Therefore, they are not easy to use in real applications. To address this issue, we can use the relative function value difference as the stopping condition based on the CCP algorithm:

$$\frac{\delta^t}{\theta^0} \leq \epsilon, \quad (24)$$

where δ^t is the function value difference between the $(t-1)$ th and t th iteration, ϵ is a small tolerance and θ^0 denotes the initial objective function value. In our problem, since $\theta^0 = \|\mathbf{b}\|^2/2$, the stopping condition becomes $2\delta^t/\|\mathbf{b}\|^2 \leq \epsilon$. Notice that this condition is applicable for those methods that cannot monotonically converge.

3.6 Convergence Analysis

At first, we show that GMP can surely converge.

Theorem 4. (Lemma 3.1 and Theorem 3.1 in [36]) *The sequence $\{\delta^t\}$ ($\delta^t \geq 0$) generated in Algorithm 1 will converge to 0. Furthermore, there exists \hat{t} , such that $\alpha^{\hat{t}-1}$ is feasible for Problem (13) and Algorithm 1 stops in the \hat{t} th iteration with $\alpha^{\hat{t}}$ to be the optimal solution (not necessarily unique) to (13).*

It is worth mentioning that the above convergence property in Theorem 4 does not require any restricted conditions. That is to say, GMP will surely converge. In addition, we can further show that GMP can exponentially converge under mild conditions. To achieve this result, we first show that, if $\lambda > 0$, the solution obtained by GMP satisfies the restricted set condition in Definition 2.

Lemma 4. *Let \mathbf{x}^* be the accumulation point of GMP with $\lambda > 0$, \mathbf{x}^* is also the optimal solution to $\min_{\mathbf{x}} \frac{1}{2}\|\mathbf{b} - \mathbf{A}\mathbf{x}\|^2 + \lambda\|\mathbf{x}\|_1$. Suppose \mathcal{T} is the support of the ground truth \mathbf{x} , let $\mathbf{h} = \mathbf{x} - \mathbf{x}^*$, then \mathbf{h} satisfies the restricted set $\Gamma_C = \{\mathbf{h} \in \mathbb{R}^m : \|\mathbf{h}_{\mathcal{T}^c}\|_1 \leq D\|\mathbf{h}_{\mathcal{T}}\|_1\}$, with $D = \frac{1+\epsilon}{1-\epsilon}$ and $\epsilon > 0$.*

From Lemma 4, with appropriate selected $\lambda > 0$, the sequence $\{\mathbf{x}^t\}$ generated by GMP will converge to the global solution of LASSO. Suppose \mathbf{x}^* is the optimal solution, $f(\mathbf{x}^*)$ is the optimal function value and \mathbf{e} is the regression error for LASSO. Let \mathcal{I}^* be the support of \mathbf{x}^* and assume $|\mathcal{I}^*| \leq k$, then $f(\mathbf{x}^t)$ will exponentially approach to $f(\mathbf{x}^*)$ if $\delta_{k+t\varrho} < 1/2$.

Theorem 5. *Let $\{\mathbf{x}^t\}$ be the sequence generated by GMP with $\lambda > 0$, we have $f(\mathbf{x}^t) \geq Cf(\mathbf{x}^*) = C(\frac{1}{2}\|\mathbf{e}\|^2 + \lambda\|\mathbf{x}^*\|_1)$, where $C > 1$. Furthermore, if $\delta_{k+t\varrho} < 1/2$ holds for $\iota > 1$, GMP can exponentially converge if $t < \iota$. Specifically, we have $f(\mathbf{x}^{t+1}) \leq \nu f(\mathbf{x}^t)$, where $\nu = \left(1 - \frac{\varrho}{4k\zeta} \left(\frac{C(1-2\delta_{(k+\iota\varrho)})^2}{(\sqrt{C}+1)^2(1-\delta_{(k+\iota\varrho)})}\right)\right)(1 - \frac{1}{C})^2$ is a constant.*

When λ is arbitrarily small (where $\lambda \geq 0$), without proper stopping conditions, GMP will converge to the point where $\|\alpha\|$ is very small. Since the regression error $\xi = \alpha$ holds, the optimal solution is meaningless for the noise cases if λ is arbitrarily small. In this sense, we suppose GMP is

stopped once \mathbf{x}^t sufficiently approaches to the ground truth k -sparse signal $\hat{\mathbf{x}}$. Let \mathbf{e} be the ground-truth additive noise, the following theorem indicates that GMP will exponentially approach to $f(\hat{\mathbf{x}}) = \frac{1}{2}\|\mathbf{e}\|^2$.

Theorem 6. *Let $\{\mathbf{x}^t\}$ be the sequence generated by GMP with arbitrarily small $\lambda(\lambda \geq 0)$, suppose $f(\mathbf{x}^t) \geq Cf(\hat{\mathbf{x}}) = \frac{C}{2}\|\mathbf{e}\|^2$ (where $C > 1$), if $\delta_{k+\iota\varrho} < 1/2$ and $t < \iota$, GMP can exponentially converge, namely $f(\mathbf{x}^{t+1}) \leq \nu f(\mathbf{x}^t)$, where $\nu = \left(1 - \frac{\varrho}{4k\zeta} \left(\frac{C(1-2\delta_{(k+\iota\varrho)})^2}{(\sqrt{C}+1)^2(1-\delta_{(k+\iota\varrho)})}\right)\right)(1 - \frac{1}{C})^2$ is a constant.*

Remark 2. *The convergence rate in the traditional CCP is unknown [36]. Therefore Theorem 5 and 6 improve the convergence result in [36]. In addition, to prove Theorem 5, the exact solution to the master problem is not necessary. Instead, a good approximation is sufficient. Furthermore, with warm-start, several iterations are enough for the inner loop. Finally, to achieve the exponential convergence rate, ϱ is desired to be several times smaller than k .*

The convergence analysis for GMP above matches the results in [27], where the geometric convergence rate of OMP type methods under restricted conditions has been revealed. However, GMP is much faster than OMP type methods in [27], [28], [29] since it can reduce the number of matrix-vector product while maintaining the geometric convergence rate. Notice that, the motivation of GMP is much different from OMP type methods. Typically, the OMP type methods are based on the loss function and it is not straightforward for them to solve model (8) with ℓ_1 -regularization (where $\lambda > 0$).

3.7 Sparse signal recovery guarantees

The sparse signal recovery conditions, which also guarantee the uniqueness of the global solution, are important in the context of compressive sensing, which is usually expressed in terms of RIP constant. Based on Lemma 4, the following recovery guarantee holds for GMP.

Theorem 7. *GMP with proper $\lambda > 0$ will recover the signals if the restricted isometry constant $\sigma_k \leq 0.307 - \nu$, where ν can be arbitrarily close to 0.*

When λ is arbitrarily small, particularly for $\lambda = 0$, a good RIP condition for the exact signal recovery is difficult to achieve, which we leave for future study. However, in practice, it has similar performance with GMP under properly selected λ , which will be shown in the experiments. By comparison, CoSaMP, SP, AIHT and OMPR can recover any k -sparse signal provided with $\delta_{4k} < 0.35$, $\delta_{3k} < 0.35$, $\delta_{3k} < 1/\sqrt{32}$ and $\delta_{2k} < 0.499$, respectively [23]. However, except AIHT, the above conditions are also the corresponding convergence guarantees. In addition, to achieve the guaranteed performance, a good estimation of the sparsity k is necessary for them, which restricts them for many applications.

4 RELATED WORK

In recent years, many fast ℓ_1 -algorithms have been developed. Among them, the alternating direction method (ADM) and the augmented Lagrange multiplier (ALM) method have shown

good performance on solving problem (3) with \mathcal{B}^2 noise; while the fast iterative shrinkage-threshold algorithm (FISTA) has shown good performance on solving the LASSO problem (4) [42]. To improve the efficiency, an elegantly designed parallel coordinate descent method, named as *Shotgun*, has been proposed [43] to improve the efficiency. Another recent work, named as S-L1, uses a screening test to predict the atoms with zero weights and reduces the computational cost with random projections [44]. Furthermore, a proximal gradient homotopy (PGH) method is proposed to solve a series of strongly convex problems by gradually decreasing the regularization parameter from an initial guess λ_0 to the target λ such that the geometric convergence rate can be maintained for each subproblem [19]. However, the efficiency of the above mentioned ℓ_1 methods is still limited due to the frequent calculations of \mathbf{Ax} and $\mathbf{A}^\top \boldsymbol{\xi}$ (both of them scales $O(mn)$). On the contrary, GMP solves the LASSO problem using a greedy strategy, and only calculates $\mathbf{A}^\top \boldsymbol{\xi}$ several times to select the most-active atoms. In addition, each master problem optimization maintains a geometric convergence rate and scales $O(|\mathcal{I}|n)$, where \mathcal{I} is the index set of the selected atoms. Therefore, with warm-start, GMP can be much more efficient than the ℓ_1 methods which needs frequent calculation of \mathbf{Ax} and $\mathbf{A}^\top \boldsymbol{\xi}$. Finally, when tackling a large number of signals with medium size m , the computational cost can be further reduced using a batch mode implementation, which will be depicted in Section 6.

5 NUMERICAL EXPERIMENTS

In this section, we will compare the performances of GMP and SGMP with the following baseline methods:

- Four well-known greedy pursuit algorithms: OMP, AIHT³, SP⁴ and OMPR are included as baseline methods. In OMPR, it needs to calculate $\mathbf{z} = \mathbf{x} + \eta \mathbf{A}^\top (\mathbf{b} - \mathbf{Ax})$, where η is learning rate [23]. The setting of η is very important for its performance [23]. In [23], a feasible range for η is provided if \mathbf{A} satisfies the RIP condition. Unfortunately, if \mathbf{A} is not well scaled, the scale of $\mathbf{A}^\top (\mathbf{b} - \mathbf{Ax})$ may vary a lot and the setting of η will be difficult⁵. Motivated by GMP, we can adaptively set η using the CGD rule. To distinguish, we name OMPR with the adaptive parameter setting as the OMPRA.
- Four state-of-the-art ℓ_1 -solvers: *Shotgun*⁶ is a fast parallel coordinate descent solver which is implemented in C++ [43]. FISTA⁷ uses the accelerated proximal gradient method with continuation technique [45], [46]; PGH⁸ uses homotopy method to improve the convergence speed [19]; S-L1⁹ adopts a screening test to predict the zero entries to improve the decoding efficiency [44].

In the experiments, *Shotgun* is conducted on Intel(R) Core(TM) i7 CPU (8 cores) with 64-bit Linux OS, while

the other methods are conducted on 64-bit Windows operating system(OS) with the same computer configuration. For fair comparisons, except S-L1, all methods are written in C++. For S-L1, which is written in Matlab, we run it in parallel mode on the multi-core machine. A Matlab interface of the C++ implementations is available on website: <https://sites.google.com/site/sparsecodingprojects/home>.

5.1 General Experimental Settings

The numerical simulation settings follow the strategy in [25], [19]. Typically, we study compressive sensing problems based on *Gaussian* random matrices of two different scales, namely, $\mathbf{A} \in \mathbb{R}^{2^{10} \times 2^{13}}$ and $\mathbf{A} \in \mathbb{R}^{2^{13} \times 2^{17}}$. In addition, three types of sparse signals, *Zero-one* signal (denoted by \mathbf{s}_z and each nonzero entry is either 1 or -1), *Uniform* signal (denoted by \mathbf{s}_u and each nonzero entry is sampled from a uniform distribution $\mathcal{U}(-1, 1)$) and *Gaussian* signal (denoted by \mathbf{s}_g and each nonzero entry is sampled from a Gaussian distribution $\mathcal{N}(0, 1)$) will be studied. The measurement \mathbf{b} is generated by $\mathbf{b} = \mathbf{Ax} + \boldsymbol{\xi}$ with *Uniform* noise sampled from $[-0.01, 0.01]$. The decoding performance and decoding time are reported to demonstrate the performance. Here the decoding performance is measured by the *empirical probability of successful reconstruction* (EPSR), which denotes the ratio of successful decoding times over M independent experiments [25]. For ℓ_1 -methods, the de-biasing technique (implemented by CGD) is used to improve the decoding performance [45], [46].

We set λ to $0.005 \|\mathbf{A}^\top \mathbf{b}\|_\infty$ for ℓ_1 methods by default, which is suggested by many ℓ_1 packages [45]. For AIHT, SP OMPR, the estimation of the sparsity \hat{k} is required. In the simulation, where we know the ground-truth k , we estimate it by $\hat{k} = 1.2k$, where k is the ground-truth. For GMP and SGMP, motivated by the fact that ℓ_1 methods can recover any k sparse signals with $n = O(k \log(m))$ measurements [1], [4], [13], we intuitively set ϱ for GMP and SGMP by

$$\varrho = n/(r \log(m)), \quad (25)$$

where $r \geq 3$. In those applications where k is known in advance, ϱ can be set by $\varrho = k/r$ with $r \geq 6$. For SGMP, we set the subspace search length parameter $\omega = 4$. The learning rate η in OMPR is set to 0.7. Finally, we stop all the algorithms once $\frac{\delta^t}{\|\mathbf{b}\|^2} \leq 1.0 \times 10^{-5}$ for fair comparisons. We keep the default settings of other parameters for baseline methods as in their original implementations.

The numerical experiments are organized into 2 parts. Firstly, the convergence properties of GMP with $\lambda > 0$ are studied. Secondly, thorough comparisons are conducted between GMP and other baseline methods.

5.2 Performance of GMP ($\lambda > 0$)

5.2.1 Influences of ϱ on GMP

In this experiment, we study the influences of ϱ on (S) GMP on *Gaussian* random matrix $\mathbf{A} \in \mathbb{R}^{2^{10} \times 2^{13}}$. Since $n/\log(m) = 113$, we set a baseline estimation for ϱ by $\rho = \lceil n/(4 \log(m)) \rceil = 28$. We also test the other two parameters: $\lceil \rho/2 \rceil$ and 2ρ . Moreover, a 160-sparse *Zero-one* vector \mathbf{x} is generated as the ground truth. Finally, PGH is adopted as the baseline method.

3. <http://www.personal.soton.ac.uk/tb1m08/publications.html>.

4. <http://sites.google.com/site/igorcarrron2/cscodes>.

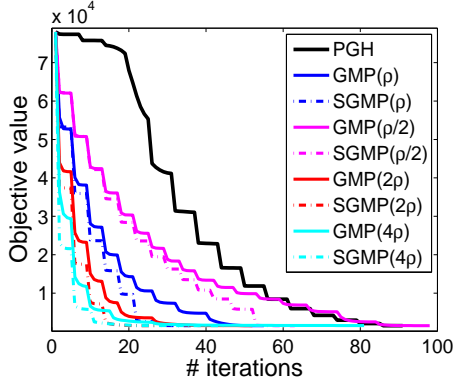
5. Interesting readers can refer to [23] for the detailed discussions on η .

6. <http://www.select.cs.cmu.edu/projects>.

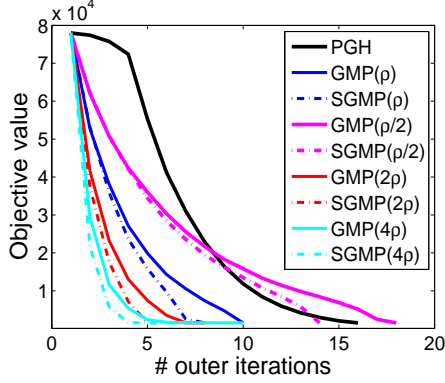
7. <http://www.eecs.berkeley.edu/~yang/software/11benchmark/index.html>.

8. <http://www.eecs.berkeley.edu/~yang/software/11benchmark/index.html>.

9. <http://www.princeton.edu/~zxiang/home/index.html>.



(a) Objective value evolution w.r.t. increasing proximal iterations.



(b) Objective value evolution w.r.t. outer iterations.

Fig. 1. Convergence properties of GMP (M1) and PGH on $\mathbf{A} \in \mathbb{R}^{2^{10} \times 2^{13}}$, where \mathbf{x} is *Zero-one* sparse vector of sparsity $\|\mathbf{x}\|_0 = 160$. For GMP (ϱ), ϱ is set to 28. The computation time (in seconds) for various methods is: 0.921, 0.172, 0.156, 0.109, 0.109, 0.124, 0.094, 0.686 and 0.219, respectively.

Fig. 1(a) and Fig. 1(b) present the objective value evolutions w.r.t. the total proximal iterations and the outer iterations, respectively. The computation time of various methods are listed in the figure caption. From Fig. 1, we have several observations. First of all, (S) GMP with different ϱ can achieve faster convergence rate than PGH. However, SGMP generally converges faster than GMP under the same ϱ , which verifies the effectiveness of subspace exploratory search. In addition, although GMP converges faster with larger ϱ at the beginning, it may have slower convergence speed at the final iterations. More critically, the total computational cost may increase a lot. For example, GMP needs 0.686 seconds to converge. The reason is that if ϱ is too large, some irrelevant atoms may be wrongly included, and the computational cost of inner problem will also increase. For smaller ϱ , although the number of outer iterations will increase, the computational cost for the inner problem is small. Accordingly, the total computational cost may be very small. Recall that GMP requires $O(mn)$ to calculate $\mathbf{A}^\top \alpha$ in each outer iteration, a good setting of ϱ that well trades off the cost of $\mathbf{A}^\top \alpha$ and the master problem optimization is important. As shown in Fig. 1, the estimation rule given in equation (25) shows promising results.

5.2.2 Influences of λ on GMP

GMP can produce different matching pursuit algorithms using arbitrarily small λ . To verify the performances of different λ , we set a baseline λ by $\lambda = 0.005 \|\mathbf{A}^\top \mathbf{b}\|_\infty$. Besides, two smaller λ , $10^{-3}\lambda$ and $10^{-6}\lambda$, are also studied. In addition, we set $\varrho = n/(4 \log(m))$ for all GMP. PGH and FISTA are adopted as the baseline methods. Two types of signals, namely the *Zero-one* signal and *Gaussian* signal are studied. For each type of sparse signal, we vary the sparsity k to obtain different sparse vectors. For each k , we run $M = 100$ independent trials.

The decoding performance and decoding time of each algorithm are reported in Fig. 2. From Fig. 2, all methods attain the similar decoding performance on *Zero-one* signals. However, GMP with various λ shows much better efficiency than PGH and FISTA. In addition, SGMP shows slightly better efficiency than GMP with larger k . On *Gaussian* signals, (S) GMP with various λ show better decoding performance than PGH and FISTA. Similar to *Zero-one* signal, GMP with various λ also show much better efficiency than PGH and FISTA for a broad range of k . Finally, SGMP also outperforms GMP in decoding performance, which verifies the effectiveness of the subspace search.

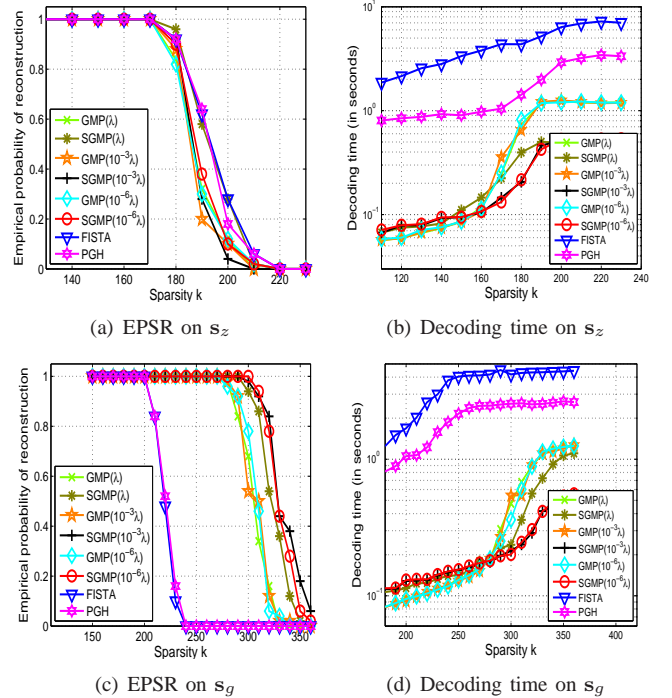


Fig. 2. Sparse reconstruction results on $\mathbf{A} \in \mathbb{R}^{2^{10} \times 2^{13}}$.

From Fig. 2, FISTA shows similar decoding performance to PGH, but attains worse efficiency in all cases. Therefore, in the following comparisons, we will exclude FISTA for space issues. At last, in order to do comparisons with other MP algorithms, only GMP with $\lambda = 0$ will be studied later, which makes no harm to the completeness of the comparison since GMP with a wide range of λ shows close performance.

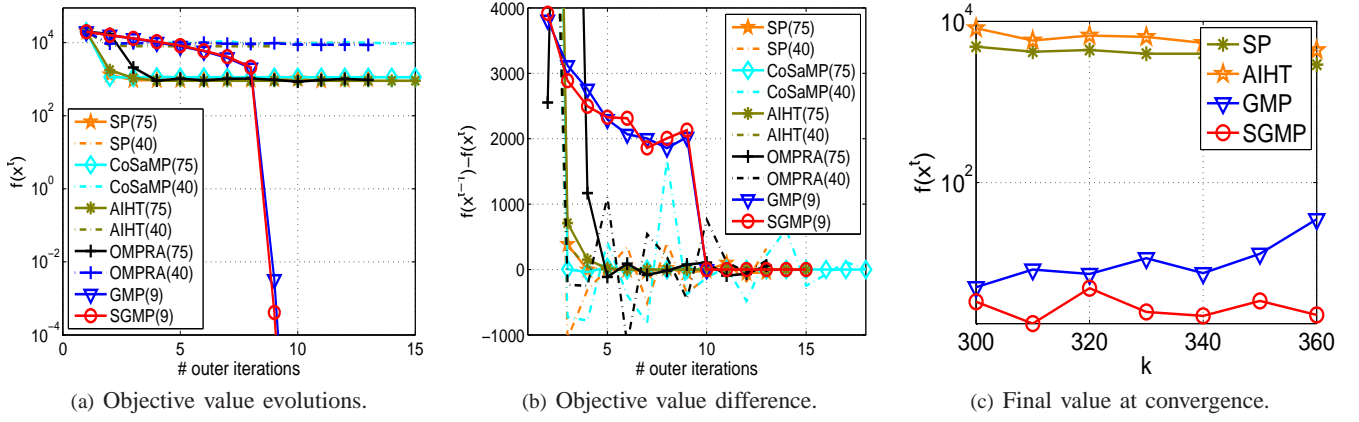


Fig. 3. Convergence comparisons on non-RIP problems. The number in bracket in Fig. 3(a) and 3(b) denotes the estimation of sparsity \hat{k} or $\hat{\rho}$. The sparsity of the solutions obtained by GMP and SGMP are both 72 when converge.

5.2.3 Convergence on Non-RIP Problems

According to Theorem 4, GMP can surely converge. On the contrary, some OMP variants only converge under restricted conditions. To demonstrate this issue, we compare the performance of GMP with SP, CoSaMP, AIHT and OMPRA on a synthetic problem, where the restricted condition does not hold. Typically, we generate an non-RIP problem by setting $\mathbf{A}(:, 41 : 80) = \mathbf{A}(:, 1 : 40)$ (in Matlab notation), where the original $\mathbf{A} \in \mathbb{R}^{2^{10} \times 2^{13}}$ is Gaussian matrix. In this case, the RIP condition does not hold since there are correlated columns in \mathbf{A} . Finally, a 40-sparse ground truth \mathbf{x} is set by letting $\mathbf{x}(1 : 40) = \mathbf{1}$ and $\mathbf{x}(41 : 8092) = \mathbf{0}$. The response vector \mathbf{b} is generated by $\mathbf{b} = \mathbf{A}\mathbf{x}$ without noise. Notice that this setting may happen in the face recognition task where similar or same images of a person can appear in \mathbf{A} for many times.

The convergence behaviors of various methods are shown in Fig. 3. From Fig. 3(a), only GMP and SGMP achieve the global solution (**not unique** in this case), while other methods can only obtain a local solution. Fig. 3(b) shows the objective value difference of successive iterations, where we can observe that, only AIHT, GMP and SGMP can monotonically decrease in objective value (since the difference is always greater than 0). The comparisons above verify the previous arguments on the convergence of the improved OMP variants, namely, these algorithms require restricted conditions to converge. On the contrary, GMP can surely converge.

To further demonstrate the convergence when RIP condition does not hold, we show an additional example on $\mathbf{A} \in \mathbb{R}^{2^{10} \times 2^{13}}$ with Zero-one signals. Here we choose large k from $\{300, 310, 320, 330, 340, 350, 360\}$ such that the RIP condition for the exact signal recovery will not hold for any algorithms. Therefore, all algorithms cannot successfully recover the original sparse vector. For simplicity, we only record the final objective value $f(\mathbf{x}^t) = \|\mathbf{b} - \mathbf{A}\mathbf{x}^t\|/2$ with different k in Fig. 3(c). From Fig. 3(c), the regression error for (S)GMP is very small, indicating that (S)GMP indeed can converge to a global solution w.r.t. α such that the regression error is minimized. On the contrary, both SP and AIHT can only get local solutions.

5.3 Sparse Recovery Performance Comparisons

In this experiment, we test the decoding performance and efficiency of all methods on a relatively small problem $\mathbf{A} \in \mathbb{R}^{2^{10} \times 2^{13}}$, where Shotgun and S-L1 work in parallel. For each k , we run $M = 100$ independent trials. The empirical probability of successful reconstructions and the decoding time for the three kinds of signals are presented in Fig. 4, where the following observation can be obtained. Firstly, on Zero-one signal, SGMP and the ℓ_1 -based methods show the best decoding performance while SP shows better decoding performances over other MP methods. Secondly, on Uniform and Gaussian signals, SGMP and OMP show relatively better decoding performance than other methods. Moreover, in all cases, SGMP shows better decoding performance than GMP. Thirdly, for AIHT, since it is easy to get stuck into local minima, it shows relatively worse decoding performance than other methods. Also, MP algorithms are faster than Shotgun, a well designed parallel ℓ_1 method. Finally, although OMPRA shows relatively better RIP condition [23], it is sensitive to its learning rate η according to our study. From the experiments, OMPRA that uses adaptive learning rate improves OMPRA greatly on all problem settings both on the decoding performance and decoding efficiency, but it is still worse than GMP and SGMP. Finally, in general, PGH shows the best efficiency than other ℓ_1 methods, such as Shotgun and S-L1, but it performs worse than (S) GMP.

In the final experiment, we focus on the scalability of various methods on a larger problem $\mathbf{A} \in \mathbb{R}^{2^{13} \times 2^{17}}$. Here only the Gaussian signals are studied. For computational issues, we only compare SP, AIHT, GMP, and SGMP with 10 trials for each parameter k . Both decoding performance and time of various methods are shown in Fig. 5. Similar observations are also obtained to the above small-scale problem. Again, GMP and SGMP achieve the best decoding performance over all methods.

6 FACE RECOGNITION BY SPARSE RECOVERY

6.1 Problem Setting

Recently, face recognition by SR has been widely studied by many researchers [2], [46], [48]. The basic assumption of SR

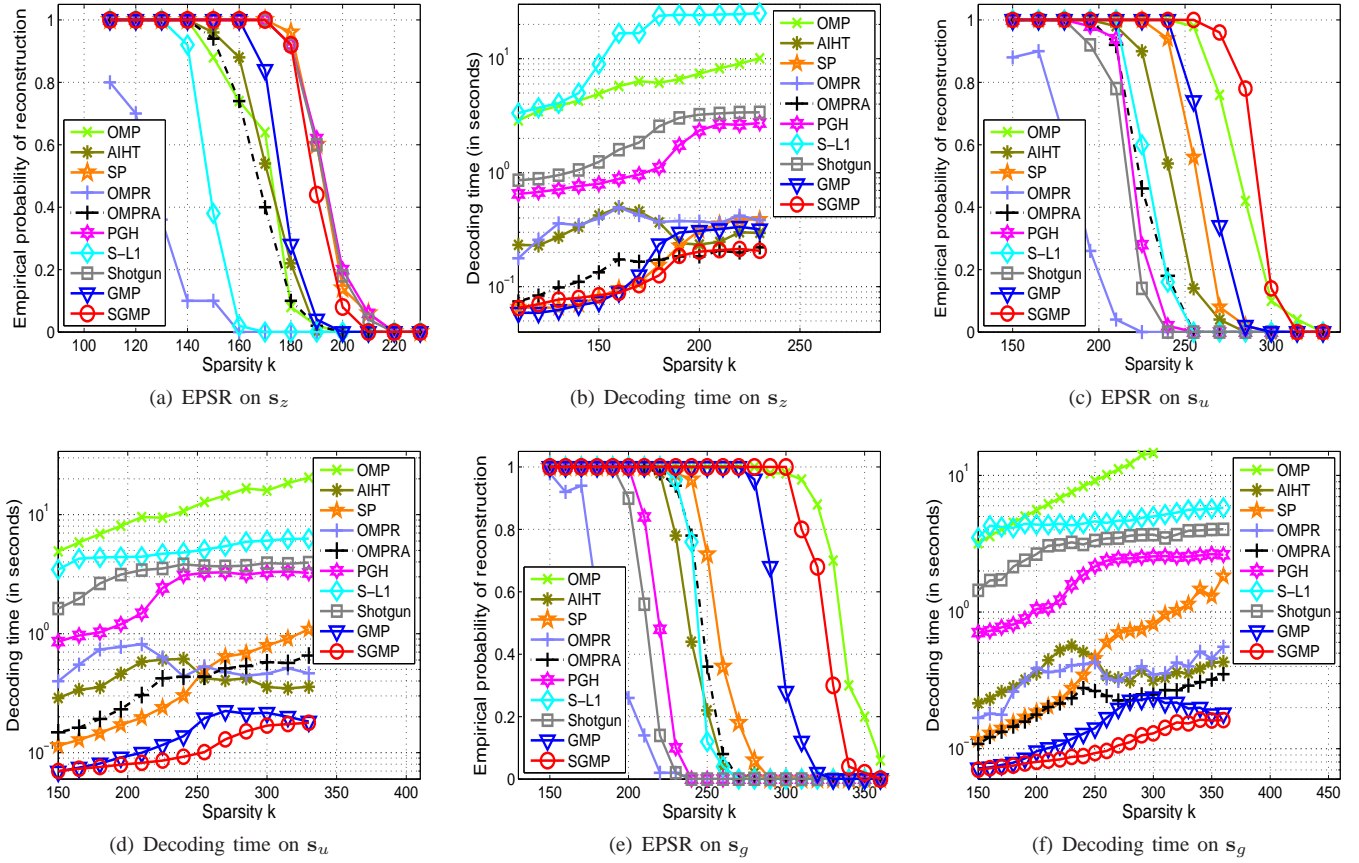


Fig. 4. Sparse recovery results on $\mathbf{A} \in \mathbb{R}^{10 \times 13}$.

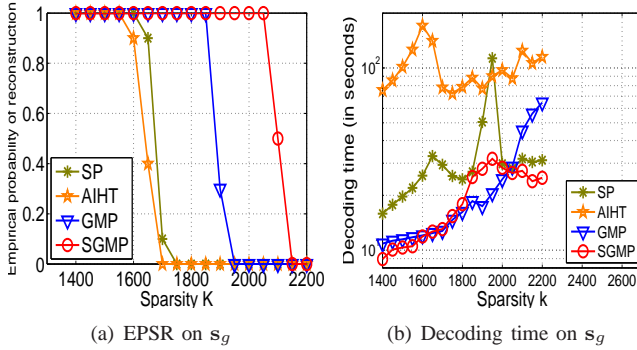


Fig. 5. Sparse recovery results on $\mathbf{A} \in \mathbb{R}^{13 \times 17}$ with Gaussian signals.

for face recognition is that any testing image lies in the subspace spanned by the training images of the same person [2], [21], [46]. As the number of training images per class is usually small, the testing image is assumed to be sparsely represented by the training images. Mathematically, given a testing image \mathbf{b} , it is assumed to be sparsely represented by the training image set $\mathbf{A} \in \mathbb{R}^{n \times m}$ by solving problem (3), where n is the number of pixels and m is the number of images. However, directly solving (3) is computationally expensive when n is very large [2], [21], [46]. To address this issue, a random matrix $\Phi \in \mathbb{R}^{q \times n} (q < n)$ is introduced to reduce the dimension of images [2].

However, several recent papers [21], [22] argued that the sparsity is not necessary on improving the recognition performance [21], [22] but increases the computational cost [20], [21]. Specifically, in [21], the authors suggested that directly solving $\|\mathbf{b} - \mathbf{A}\mathbf{x}\|^2$ without any dimension reduction, denoted as L2, can achieve better recognition rates and faster predictions; while in [22], the authors showed that solving a least square problem $\|\mathbf{b} - \mathbf{A}\mathbf{x}\|^2 + \frac{\lambda}{2}\|\mathbf{x}\|^2$, denoted by L2-L2, can achieve better recognition rates. The efficiency of L2 and L2-L2 is the major advantage over SR. In L2, since $\mathbf{x} = \mathbf{R}^{-1}\mathbf{Q}^\top\mathbf{b}$, one can pre-compute $\mathbf{R}^{-1}\mathbf{Q}^\top$ and store it in memory, where $\mathbf{A} = \mathbf{QR}$ denotes the QR decomposition and \mathbf{R}^{-1} denotes the pseudo inverse. Then fast predictions can be achieved using simple matrix-vector product. Similarly, in L2-L2, as $(\mathbf{A}^\top\mathbf{A} + \lambda\mathbf{I})^{-1}$ can be pre-computed, the solution $\mathbf{x} = (\mathbf{A}^\top\mathbf{A} + \lambda\mathbf{I})^{-1}\mathbf{A}^\top\mathbf{b}$ can be calculated very quickly. The second critical issue for ℓ_1 -method is the difficulty on the trade-off setting between sparsity and reconstruction error $\|\mathbf{b} - \mathbf{A}\mathbf{x}\|^2$ by tuning the parameter λ [20]. Without proper setting of λ , the enforcing of high sparsity may even degrade the performance [21], [20]. Regarding these issues, two questions are raised.

- Can we reduce the difficulty of the trade-off parameter settings in ℓ_1 methods?
- Does sparsity really help to improve the performance?

Before answering the above questions, we first introduce the batch-mode implementation of GMP.

6.2 Batch Mode GMP

Recall that L2 and L2-L2 methods pre-compute the matrix inverse (or pseudo-inverse) to achieve fast predictions for a batch of testing images. The question is: can we do the similar implementations for GMP?

Recall that, in GMP, the master problem scales $O(|\mathcal{I}|n)$ complexity and the worst-case analysis scales $O(mn)$, where \mathcal{I} is the index set of the selected atoms. Apparently, the worst-case analysis dominates the complexity of the whole algorithm if n is very large. Fortunately, motivated by [47], this computation burden can be significantly reduced using a batch-mode implementation BGMP. Notice that $\mathbf{A}^\top \boldsymbol{\alpha} = \mathbf{A}^\top (\mathbf{b} - \mathbf{A}_{\mathcal{I}} \mathbf{x}_{\mathcal{I}})$ can be calculated via

$$\mathbf{A}^\top \boldsymbol{\alpha} = [\mathbf{A}^\top \mathbf{b}] - [\mathbf{A}^\top \mathbf{A}_{\mathcal{I}}] \mathbf{x}_{\mathcal{I}}. \quad (26)$$

If we pre-compute $[\mathbf{A}^\top \mathbf{b}]$ and $\mathbf{Q} = \mathbf{A}^\top \mathbf{A}$ and store them in the memory, we can calculate $\mathbf{A}^\top \boldsymbol{\alpha}$ by $\mathbf{A}^\top \boldsymbol{\alpha} = [\mathbf{A}^\top \mathbf{b}] - \mathbf{Q}_{\mathcal{I}} \mathbf{x}_{\mathcal{I}}$, where $\mathbf{Q}_{\mathcal{I}}$ denotes the columns of \mathbf{Q} indexed by \mathcal{I} . Now the computational cost for $\mathbf{A}^\top \boldsymbol{\alpha}$ reduces to $O(m|\mathcal{I}|)$, which will save a lot of computation when $k \ll n$ [47]. With this strategy, when there are a lot of signals to be decoded, the computational cost can be much reduced. However, since $\mathbf{A}^\top \mathbf{A}$ needs $O(m^2)$ space for storage, this strategy is only applicable for medium size problems. If m is extremely large, \mathbf{Q} will be too large to store. In this case, one cannot store the matrix inverse for L2-L2 and L2, either.

To verify the effectiveness of BGMP, we firstly compare its performance with BOMP, which also uses the batch-mode implementation [47]. In the simulation, we generate a *Gaussian* random matrix $\mathbf{A} \in \mathbb{R}^{2^{12} \times 2^{14}}$. In addition, we generate *Gaussian* sparse signals with sparsity k from $\{400, 450, 500, 550, 600\}$. For each k , 200 sparse signals are generated. Finally, the measurements \mathbf{b} is produced by $\mathbf{b} = \mathbf{A}\mathbf{x} + \boldsymbol{\xi}$ with *Gaussian* noise sampled from $\mathcal{N}(0, 0.05)$. The total time (in seconds) spent by BGMP and BOMP on 200 signals as well as the Mean Square Error (MSE) are reported in Table 1. Table 1 shows that BGMP is about 7-16 times faster than BOMP. Moreover, it gains better or comparable MSE than BOMP for all k .

TABLE 1
Efficiency Comparison Between BGMP and BOMP

	k	400	450	500	550	600
BOMP	Time	434.27	546.70	680.96	835.72	1014.93
	MSE	8.61E-04	9.89E-04	1.11E-03	1.25E-03	1.40E-03
BGMP	Time	55.06	55.79	56.79	59.51	59.91
	MSE	3.72E-04	3.55E-04	3.40E-04	3.49E-04	3.38E-04
	Speedup	7.89	9.80	11.99	14.04	16.94

6.3 Experimental Results

Now we apply BGMP to face recognition. In addition, since thorough comparisons between ℓ_1 methods and other methods have been done in [2], [46], [48], in this experiments, we only adopt L2 and L2-L2, PGH and BOMP as the baseline methods. Notice that those MP algorithms that require an exact guess of k , such as SP and OMPR, are not suitable for face recognitions. Two reasons account for this. Firstly, for general problems, it is difficult to set k . On the one hand, if k is too small, the reconstruction error will be large and the performance will

degrade. On the other hand, if k is too large, the computational cost will increase. Secondly, the training image set \mathbf{A} may not satisfy the RIP conditions, hence these algorithms may not converge or only converge to a local solution.

Two widely used databases, namely, the *Extended using* and *AR* database are studied. The *Extended using* consists of 2,414 frontal face images of 38 subjects [21], [48]. They are captured under various lighting conditions and cropped and normalized to 192×168 pixels. In our experiment, we take 62 images per person, resulting 2,356 images in total. The *AR* dataset consists of over 2,600 frontal images of 100 individuals [49], [2], [48]. Each image is normalized to 80×60 pixels. We set the stopping condition $\|\mathbf{b} - \mathbf{A}\mathbf{x}\|^2 / \|\mathbf{b}\|^2 \leq 10^{-6}$ for BGMP and $k = 200$ for BOMP. Furthermore, considering that there may be some images that cannot be sparse-represented by the training images, we constrain the sparsity $k \leq 600$. Finally, since the number of measurements n can be very large, the estimation of ϱ in equation (25) is not suitable. Therefore, we directly set $\varrho = 10$ for all experimental settings.

6.3.1 Face Recognition with Different Dimensions

Followed by [21], we randomly choose half images of each person as training set and the rest images as testing set. To study the influence brought by the number of measurements (pixels), we down-sample the images with sampling rate ρ_d , where ρ_d is chosen from $\{1, 1/2, 1/3, 1/4, 1/5, 1/6, 1/7\}$ for *YaleB* images and $\{1, 3/4, 2/3, 1/2, 1/3\}$ for *AR* images. Obviously, the dimension of new image vector will be ρ_d^2 of the original image vector. The prediction accuracies on *YaleB* and *AR* images are shown in Table 2. To measure the difference of the result, the *Wilcoxon* test with 5% significance is conducted between BGMP and the winner of L2 and L2-L2, and 1 indicates the significant difference.

From Table 2, we can observe that, on *YaleB* dataset, BGMP shows significantly better accuracy than L2 and L2-L2 methods under down-sampling rate $1/5, 1/6$ and $1/7$ and comparable or slightly better performance under other down-sampling rates. On *AR* dataset, BGMP performs significantly better than L2 and L2-L2 under down-sampling rate $1, 3/4$ and $2/3$. Moreover, BGMP and BOMP can achieve more stable performance on a wide range of down-sampling rates than L2 and L2-L2. For L2 method, it shows very unstable performance under some sampling rates. For example, on *AR* dataset, it only achieves **73.23%** testing accuracy under down-sampling rate $1/2$. The possible reason is the unstable pseudo inverse on ill-conditioned matrix. Its performance can be possibly stabilized by adding a regularization term $\lambda \mathbf{I}$ to $\mathbf{A}^\top \mathbf{A}$, namely L2-L2. From Table 2, L2-L2 indeed shows better stable performance under different sampling rates than L2-L2. But it performs worse than BGMP and BOMP on *AR* database with large number of measurements.

The major complaint for ℓ_1 methods is their unbearable time cost [2], [46], [21]. To demonstrate the efficiency, we report the total time spent by various methods in Table 3. From Table 3, without down-sampling, PGH, the considered state-of-the-art ℓ_1 solver, needs several hours to predict all testing images, which is unbearable for real-world applications. However, BGMP can finish the prediction within one minute, which is

TABLE 2
Prediction Accuracy on Two Databases

ρ_d	Extended YaleB Database							AR Database				
	1	1/2	1/3	1/4	1/5	1/6	1/7	1	3/4	2/3	1/2	1/3
L2	0.9876	0.9868	0.9831	0.9792	0.9371	0.9561	0.9621	0.9466	0.9301	0.9108	0.7323	0.9638
L2-L2	0.9898	0.9859	0.9827	0.9818	0.9783	0.9730	0.9723	0.9524	0.9504	0.9532	0.9574	0.9692
PGH	0.9897	0.9843	0.9826	0.9846	0.9815	0.9760	0.9658	0.9657	0.9650	0.9715	0.9679	0.9656
BOMP	0.9904	0.9897	0.9861	0.9844	0.9786	0.9799	0.9734	0.9742	0.9744	0.9738	0.9738	0.9619
BGMP	0.9911	0.9892	0.9873	0.9849	0.9817	0.9787	0.9761	0.9739	0.9757	0.9715	0.9723	0.9672
Wilcoxon	0	0	0	0	1	1	1	1	1	1	1	0

TABLE 3
Total Time Spent on Two Databases (in seconds)

ρ_d	Extended YaleB Database							AR Database				
	1	1/2	1/3	1/4	1/5	1/6	1/7	1	3/4	2/3	1/2	1/3
L2	71.33	24.91	6.29	3.51	2.42	1.14	0.72	13.34	4.39	3.16	3.28	2.19
L2-L2	11.36	6.85	4.13	2.40	2.32	2.22	1.69	3.75	3.04	3.10	2.58	1.99
PGH	5559.53	4863.18	2195.03	1383.28	822.11	627.95	383.86	5229.75	2812.96	2178.91	1324.59	557.65
BOMP	139.69	99.88	98.05	89.83	89.95	90.41	87.60	108.52	98.84	98.60	97.25	95.58
BGMP	39.72	17.05	12.94	7.86	7.62	6.53	6.19	14.29	10.87	10.20	7.14	4.57

TABLE 4
Average Sparsity on Two Databases

ρ_d	Extended YaleB Database							AR Database				
	1	1/2	1/3	1/4	1/5	1/6	1/7	1	3/4	2/3	1/2	1/3
BOMP	200	200	200	200	200	200	200	200	200	200	200	200
PGH	164	165	165	162	156	158	163	133	130	127	135	124
BGMP	167	165	160	155	155	149	143	189	190	188	194	201

comparable with L2-L2 and L2. Particularly, BGMP can be up to 500 times faster than PGH [19], and it also performs 3-10 times faster than BOMP method. That is to say, under fair implementations in batch mode, BGMP can achieve the comparative efficiency with L2-L2 and L2.

The remaining question is: does the sparsity help to improve the recognition performance? To answer this question, we listed the average sparsity of BGMP, PGH, and BOMP in Table 4. Notice that the solutions obtained by L2 and L2-L2 are not sparse. From Table 4, BGMP, PGH and BOMP indeed achieve sparse solutions. However, BGMP shows better prediction accuracy than PGH method by directly controlling the reconstruction error $\|\mathbf{Ax} - \mathbf{b}\|^2$. Moreover, from Table 4, BOMP has larger number of nonzeros than BGMP in most case, but it does not show much improved prediction accuracy over BGMP. Therefore, we can conclude that the preserving of the sparsity at least **does not degrade** the performance if we control the reconstruction error $\|\mathbf{Ax} - \mathbf{b}\|^2$ to be small enough. More importantly, on AR dataset, BGMP outperforms L2 and L2-L2 with enough measurement (pixels), therefore, the sparsity indeed **help to improve** the recognition rates on AR dataset.

6.3.2 Face Recognition with Different Training Samples

To further demonstrate whether the sparsity can help to improve the recognition rates or not, an additional experiment on YaleB database is conducted. Recall that in Table 2, when half images are used as the training set, BGMP does not perform significantly better than L2 and L2-L2 on YaleB database under the down-sampling rate $\rho_d = 1/4$. **But what will happen if the number of training images increases?** Notice that with more training images, the matrix $\mathbf{A}^\top \mathbf{A}$ will become more ill-conditioned. Let ρ_t be the ratio of the training image number

TABLE 5
Prediction Accuracy on YaleB with Different Number of Training Images

ρ_t	0.55	0.60	0.65	0.70	0.75	0.80
L2	0.6352	0.9350	0.9330	0.9684	0.9764	0.9815
L2-L2	0.9814	0.9814	0.9823	0.9827	0.9843	0.9872
BGMP	0.9848	0.9887	0.9887	0.9908	0.9911	0.9925
Wilcoxon	0	1	1	1	1	1

over the total image number, then the ratio of the testing images will be $1 - \rho_t$. To demonstrate the performance with different number of training images, we fix the down-sampling rate $\rho_d = 1/4$ and vary $\rho_t \in \{0.55, 0.60, 0.65, 0.7, 0.75, 0.8\}$. Here the dimension of each image vector is 2016, 16 times smaller than the original image vector.

The prediction accuracy and the total time spent with different number of training images are shown in Table 5 and 6, respectively. From Table 5, BGMP performs significantly better than L2 and L2-L2 when $\rho_t \geq 0.60$, which indicates that BGMP can achieve more stable performance when $\mathbf{A}^\top \mathbf{A}$ becomes more ill-conditioned. Accordingly, we can conclude that the sparsity can **help improve** the recognition rates in this setting. Again in Table 6, the total time spent by BGMP is comparable to L2 and L2-L2.

TABLE 6
Total Time Spent on YaleB with Different Number of Training Images (in seconds)

ρ_t	0.55	0.60	0.65	0.70	0.75	0.80
L2	2.48	2.95	3.02	3.16	3.56	6.02
L2-L2	2.20	2.51	3.50	3.94	3.21	6.06
BGMP	10.65	6.11	5.71	4.93	4.23	2.85

7 CONCLUSIONS

In this paper, a new convex relaxation scheme for sparse recovery problem is proposed by introducing a 0-1 support selection vector. Based on the new convex formulation, a general matching pursuit (GMP) algorithm which can surely converge is naturally introduced. It shows that GMP can converge exponentially if $\sigma_{k+t\varrho} < 0.5$. In addition, GMP with an ℓ_1 -regularizer can recover the k -sparse signals if the restricted isometry constant $\sigma_k \leq 0.307 - \nu$, where ν can be arbitrarily close to 0. Finally, SGMP with subspace search can further improve the performance of GMP. In general, GMP can be much faster than traditional ℓ_1 methods. Furthermore, the computational cost can be further reduced by using batch-mode implementation.

As a matching pursuit algorithm, GMP differs from OMP variants in several aspects. At first, GMP is motivated by solving a convex QCQP problem with the central cutting plane algorithm [36]. Therefore, it can surely converge and the global convergence is also guaranteed. On the contrary, except AIHT and OMP, most of them need restricted conditions for convergence. For AIHT, although it can monotonically decrease in objective value, experiments show that it is easy to get stuck into local minima [31], [32]. In addition, the standard OMP is a special case of GMP but with unbearable computation cost for large k . The computation issue also exist for other OMP type methods as they only include one element each iteration [28], [29]. Secondly, unlike most of the OMP variants, such as CoSaMP, SP and OMPR [24], [25], [23], GMP dose not need to specify an exact estimation of the target sparsity. Thirdly, ROMP, SP, CoSaMP and OMPR need the replacement of atoms [30], [25], [23], while GMP gradually increases ϱ atoms without any atom replacement. Finally, SGMP that uses subspace search can further improve the performance of GMP, which shares the similar strength with SP. However, they are different since SP includes additional k atoms at each iteration [25] while SGMP only need to include $\eta\varrho$ ($\eta\varrho < k$) atoms.

Comprehensive numerical experiments demonstrate the effectiveness and efficiency of the proposed methods. In addition, by applying GMP to face recognition, the experimental results on two widely used datasets, namely *Extended YaleB* Database and *AR* database, show that the batch mode GMP can achieve significantly better recognition rates than two competitors, namely L2 and L2-L2, on a wide range of settings with comparable computational cost. Particularly, batch mode GMP can be up to 20 times faster than batch-mode OMP and 500 times faster than the considered state-of-the-art ℓ_1 method, namely PGH [19].

REFERENCES

- [1] D. Donoho., "Compressed sensing," *IEEE Trans. on Information Theory*, vol. 52(4), pp. 1289–1306, 2006.
- [2] J. Wright, A. Yang, A. Ganesh, S. Sastry, and Y. Ma, "Robust face recognition via sparse representation," *IEEE Trans. on PAMI*, vol. 31(2), pp. 210–227, 2009.
- [3] A. Coates and A. Ng, "The importance of encoding versus training with sparse coding and vector quantization," in *ICML*, 2011.
- [4] E. J. Candès and T. Tao., "Decoding by linear programming," *IEEE Trans. Info. Theory*, pp. 4203–4215, 2005.
- [5] J. Mairal, M. Elad, and G. Sapiro, "Sparse representation for color image restoration," *IEEE Trans. on Image Processing*, vol. 17(1), pp. 53–69, 2008.
- [6] J. Mairal, F. Bach, J. Ponce, G. Sapiro, and A. Zisserman, "Non-local sparse models for image restoration," in *ICCV*, 2009.
- [7] J. Yang, J. Wright, T. Huang, and Y. Ma, "Image super-resolution via sparse representation," *IEEE Transactions on Image Processing*, vol. 19(11), pp. 2861–2873, 2010.
- [8] E. Elhamifar and R. Vidal, "Sparse subspace clustering," in *CVPR*, 2009.
- [9] A. Adler, M. Elad, and Y. Hel-Or, "Fast subspace clustering via sparse representations," Department of Computer Science, Technion, Tech. Rep., 2011.
- [10] J. Mairal, F. Bach, J. Ponce, and G. Sapiro, "Online dictionary learning for sparse coding," in *ICML*, 2009.
- [11] L. Bo, X. Ren, and D. Fox, "Hierarchical matching pursuit for image classification: Architecture and fast algorithms," in *NIPS*, 2011.
- [12] K. Yu, Y. Lin, and J. Lafferty, "Learning image representations from the pixel level via hierarchical sparse coding," in *CVPR*, 2011.
- [13] E. J. Candès, J. Romberg, and T. Tao, "Stable signal recovery from incomplete and inaccurate measurements," *Comm. Pure Appl. Math*, vol. 59, pp. 1207–1223, 2006.
- [14] D. Ge, X. Jiang, and Y. Ye, "A note on the complexity of lp minimization," *Math. Programming*, vol. 129(2), pp. 285–299, 2011.
- [15] B. Efron, T. Hastie, I. Johnstone, and R. Tibshirani., "Least angle regression," *Ann. Statist.*, vol. 32, pp. 407–499, 2004.
- [16] H. Lee, A. Battle, R. Raina, and A. Y. Ng., "Efficient sparse coding algorithms," in *NIPS*, 2006.
- [17] T. T. Cai, L. Wang, and G. Xu., "New bounds for restricted isometry constants," *IEEE Trans. Info. Theory*, vol. 56(9), pp. 4388–4394, 2010.
- [18] E. J. Candès and T. Tao, "Rejoinder: the dantzig selector: statistical estimation when p is much larger than n," *Annals of Statistics*, vol. 35, pp. 2392–2404, 2007.
- [19] L. Xiao and T. Zhang, "A proximal-gradient homotopy method for the l1-regularized least-squares problem," in *ICML*, 2012.
- [20] R. Rigamonti, M. A. Brown, and V. Lepetit, "Are sparse representations really relevant for image classification?" in *CVPR*, 2011.
- [21] Q. Shi, A. Eriksson, A. v. d. Hengel, and C. Shen, "Is face recognition really a compressive sensing problem?" in *CVPR*, 2011.
- [22] L. Zhang, M. Yang, and X. Feng, "Sparse representation or collaborative representation: Which helps face recognition?" in *ICCV*, 2011.
- [23] P. Jain, A. Tewari, and I. S. Dhillon, "Orthogonal matching pursuit with replacement," in *NIPS*, 2011.
- [24] D. Needell and J. Tropp, "Cosamp: Iterative signal recovery from incomplete and inaccurate samples," *Applied and Computational Harmonic Analysis*, vol. 26(3), pp. 301–321, 2009.
- [25] W. Dai and O. Milenkovic., "Subspace pursuit for compressive sensing signal reconstruction," *IEEE Trans. Info. Theory*, vol. 55(5), pp. 2230–2249, 2009.
- [26] T. Zhang, "Sparse recovery with orthogonal matching pursuit under RIP," *IEEE Trans. Info. Theory*, vol. 57, pp. 6215–6221, 2011.
- [27] S.-S. S., N. Srebro, and T. Zhang, "Trading accuracy for sparsity in optimization problems with sparsity constraint," *SIAM Journal on Optimization*, vol. 20, p. 2807C2832, 2010.
- [28] A. Tewari, P. Ravikumar, and I. S. Dhillon, "Greedy algorithms for structurally constrained high dimensional problems," in *NIPS*, 2011.
- [29] X., Yuan, and S. Yan, "Forward basis selection for sparse approximation over dictionary," in *AISTATS*, 2012.
- [30] D. Needell and R. Vershynin, "Uniform uncertainty principle and signal recovery via regularized orthogonal matching pursuit," *Journal Foundations of Computational Mathematics*, vol. 9(3), pp. 317–334, 2009.
- [31] T. Blumensath and M. E. Davies, "Iterative thresholding for sparse approximations," *The Journal of Fourier Analysis and Applications*, vol. 14(5), pp. 629–654, 2008.
- [32] T. Blumensath, "Accelerated iterative hard thresholding," *Signal Processing*, vol. 92, pp. 752–756, 2011.
- [33] R. Giryes and M. Elad., "RIP-based near-oracle performance guarantees for subspace-pursuit, cosamp, and iterative hard-thresholding," *IEEE Trans. on Signal Processing*, vol. 60(3), pp. 1465–1468, 2012.
- [34] L. Wang, "L1 penalized lad estimator for high dimensional linear regression," MIT, Tech. Rep., 2012.
- [35] E. Y. Pee and J. O. Royset, "On solving large-scale finite minimax problems using exponential smoothing," *J. Optimization Theory and Applications*, vol. 148(2), pp. 390–421, 2011.
- [36] K. O. Kortanek and H. No, "A central cutting plane algorithm for convex semi-infinite programming problems," *SIAM J. on Optimization*, vol. 3(4), pp. 901–918, 1993.

- [37] J. Elzinga and T. G. Moore, "A central cutting plane algorithm for the convex programming problem," *Math. Programming*, vol. 8, pp. 134–145, 1975.
- [38] Y. Nesterov, "Gradient methods for minimizing composite objective function," Center for Operations Research and Econometrics (CORE), Catholic University of Louvain (UCL), Tech. Rep., 2007.
- [39] B. Beckermann and A. B. J. Kuijlaars, "Superlinear convergence of conjugate gradients," *SIAM Journal on Numerical Analysis*, vol. 39(1), pp. 300–329, 2002.
- [40] E. J. Candès and Y. Plan, "Near-ideal model selection by ℓ_1 minimization. , ," *Annals of Statistics*, vol. 37, pp. 2145–2177, 2007.
- [41] T. T. Cai and L. Wang, "Orthogonal matching pursuit for sparse signal recovery with noise," *IEEE Trans. Info. Theory*, vol. 57(7), pp. 4680–4688, 2011.
- [42] A. Beck and M. Teboulle, "A fast iterative shrinkage-thresholding algorithm for linear inverse problems," *SIAM J. on Imaging Sciences*, vol. 2(1), pp. 183–202, 2009.
- [43] J. K. Bradley, A. Kyrola, D. Bickson, and C. Guestrin., "Parallel coordinate descent for ℓ_1 -regularized loss minimization," in *ICML*, 2011.
- [44] Z. J. Xiang, H. Xu, and P. J. Ramadge., "Learning sparse representations of high dimensional data on large scale dictionaries," in *NIPS*, 2012.
- [45] M. A. T. Figueiredo, R. D. Nowak, and S. J. Wright, "Gradient projection for sparse reconstruction: Application to compressed sensing and other inverse problems," *IEEE Journal of Selected Topics in Signal Processing: Special Issue on Convex Optimization Methods for Signal Processing*, 2007.
- [46] A. Yang, A. Ganesh, Y. Ma, and S. Sastry, "Fast ℓ_1 -minimization algorithms and an application in robust face recognition: A review," in *ICIP*, 2010.
- [47] R. Rubinstein, M. Zibulevsky, and M. Elad, "Efficient implementation of the k-svd algorithm using batch orthogonal matching pursuit," Technion, Tech. Rep., 2008.
- [48] S. Gao, I. W. Tsang, and L. Chia, "Sparse representation with kernels," *To appear in IEEE Transactions on Image Processing.*, 2013.
- [49] A. Martinez and R. Benavente, "The ar face database," CVC Tech, Tech. Rep., 1998.

